

Article

The Use of Key Enabling Technologies in the Nearly Zero Energy Buildings Monitoring, Control and Intelligent Management

José Marco Lourenço ^{1,*}, Laura Aelenei ¹ , Jorge Facão ¹, Helder Gonçalves ¹, Daniel Aelenei ^{2,3} 
and João Murta Pina ^{2,3}

¹ Laboratório Nacional de Energia e Geologia (LNEG), 1649-038 Lisboa, Portugal; laura.aelenei@lneg.pt (L.A.); jorge.facao@lneg.pt (J.F.); helder.goncalves@lneg.pt (H.G.)

² NOVA School of Science and Technology, NOVA University of Lisbon, 2829-516 Caparica, Portugal; aelenei@fct.unl.pt (D.A.); jmpp@fct.unl.pt (J.M.P.)

³ Center of Technology and Systems/UNINOVA, FCT Campus, 2829-516 Caparica, Portugal

* Correspondence: jose.lourenco@lneg.pt; Tel.: +351-21-092-4600 (ext. 4342)

Abstract: The 2018 revision of the European Performance Building Directive (EPBD) requires that from the year 2020 onwards, all new buildings will have to be “nearly zero energy buildings”. It also further promotes smart building technologies, raising awareness amongst building owners and occupants of the value behind building automation. The European Commission also identified, in 2011, Key Enabling Technologies (KETs), which provide the basis for innovation in the EU. In the frame of the SUDOKET project, the Solar XXI building was used as a pilot case, as innovative integrated solutions and technologies are monitored and controlled. The objective of this paper is to validate a simulation of the laboratorial test room in EnergyPlus with data obtained experimentally and determine the impact of the control systems on energy needs and on thermal comfort. Two systems, in particular, were studied: the Building-Integrated Photovoltaic (BIPV) and the earth tubes. Once validated, the simulation of the test room without the systems was created, allowing their impact to be determined. The results show that, for the analysed periods, BIPVs reduced the heating consumption by 22% while also increasing thermal comfort, and the earth tube system would reduce the cooling needs by 97%.

Keywords: key enabling technologies; smart buildings; building monitoring; control; building management; nZEB; building simulation



Citation: Lourenço, J.M.; Aelenei, L.; Facão, J.; Gonçalves, H.; Aelenei, D.; Pina, J.M. The Use of Key Enabling Technologies in the Nearly Zero Energy Buildings Monitoring, Control and Intelligent Management. *Energies* **2021**, *14*, 5524. <https://doi.org/10.3390/en14175524>

Academic Editor:
Alessandro Cannavale

Received: 6 August 2021
Accepted: 30 August 2021
Published: 4 September 2021

Publisher's Note: MDPI stays neutral with regard to jurisdictional claims in published maps and institutional affiliations.



Copyright: © 2021 by the authors. Licensee MDPI, Basel, Switzerland. This article is an open access article distributed under the terms and conditions of the Creative Commons Attribution (CC BY) license (<https://creativecommons.org/licenses/by/4.0/>).

1. Introduction

In the European Union, buildings are responsible for approximately 40% of the energy consumption and 36% of the greenhouse gas emissions [1]. In 2010, the Energy Performance of Buildings Directive (EPBD) recast [2] introduced new requirements with the objective of attaining environmental and energy efficiency goals and produce innovative and efficient buildings. Along with the Energy Efficiency Directive (EED), the two directives aimed to significantly improve the buildings in the EU, not only from an energetic point of view but also from an environmental perspective [2]. In both directives, special attention is also paid to public buildings in terms of energy efficiency measures, drivers and barriers [3] and their optimal calculation [4]. In 2018, EPBD was updated in order to convey the improvement of European buildings, in which it demands that all new public buildings be nearly Zero Energy Buildings (nZEB) by 31 December 2018, and all new buildings be nZEB by 31 December 2020 [2]. Furthermore, it aims to promote smart building technologies through a smart readiness indicator (SRI), which estimates the capability of a building to adapt its operation to the occupant's needs while optimising energy efficiency and overall performance [5]. For a building to be considered nZEB, it must reduce its energy consumption

and produce energy from renewable sources, which can compensate for the majority of the building's consumption [6] without jeopardising the occupant's thermal comfort.

In addition to these, in 2011, the European Commission identified Key Enabling Technologies (KET), a group of six technologies considered to be fundamental for Europe's industrial modernisation [7]. This group of technologies is composed of: advanced manufacturing, advanced materials and nanotechnologies, life-Science, micro-/nanoelectronics and photonics, artificial intelligence and security and connectivity [8].

Building performance solutions are known; however, their applicability and cost-effectiveness vary significantly [4], as each building's location, surroundings, and use are unique. To minimise building's consumption, an integrated solution encompassing several solutions is required, often limited by economic, social and environmental constraints. When proposing a singular solution to a particular issue, due to the interactivity in buildings, the proposed solution can provoke an undesired response, mitigating its effectiveness [9]. Additionally, individually tackling singular problems can lead to significant oversizing of the solutions and friction between them. In order to reduce this issue, solution packages are presented by examining buildings as a whole.

A method to assess buildings holistically is through building simulation, such as TRNSYS and EnergyPlus [10]. These tools allow to digitally recreate buildings alongside their surroundings and operational regimes in order to simulate the building's response to potential solutions. Santamouris et al. [11], with the aid of TRNSYS, studied the application of green roofs in nursery school buildings in Athens, concluding that the green roof would decrease the cooling load (15–49% for a non-insulated building and 6–33% for an insulated building), with increased impact on the top floor, without significantly increasing the heating load. Chidiac et al. [12] assessed the difference between the application of individual retrofit measures with a whole-building simulation on representative buildings using EnergyPlus. The study found that the sum of singular retrofit measures would overpredict the impact on energy savings.

Despite the effectiveness of building simulation programs, there is a discrepancy between the designed energy consumption and the actual registered energy consumption, denominated as building energy performance gap, which is typically within 30% [13,14]. A cause for the performance gap is occupant behaviour, as occupant actions can mitigate the building performance. Owens and Wilhite [15] conducted a survey which showed that 10–20% of the domestic energy use in Nordic countries could be reduced from occupant behavioural changes.

In order to reduce the impact of unwarranted user actions, in the course of becoming smart buildings, buildings are deploying automated control systems, which monitor the several variables influencing occupant thermal comfort and energy consumption and adjust the control systems to optimally regulate indoor air environment and power consumption for the user, such as light dimming, shading and ventilation. By implementing sensors that detect occupant presence, a significantly large share of energy can be saved, particularly in HVAC and lighting [16]. However, if an automated system is implemented without fully assessing and predicting its impact on user comfort, the system can lead to occupant dissatisfaction and control override [17].

The project SUDOKET was launched in 2018 with the objective of promoting European development and technological leadership in the subject of innovative buildings through the research, innovation and development of KET-based solutions [18]. The project developed tools that, besides being informative, allow the collaboration of participating agents. In this project, there are four demonstrators: KETmaterials, KETsupply, KETstorage and KEToperation. The present study focuses on KEToperation, demonstrating the application of KETs in monitoring, control and smart management of a test room, regarding its energy consumption and occupant thermal comfort, whose conclusions contribute to the development and promotion of KETs in the building sector.

The scientific relevance of this study, other than the specific objectives of the SUDOKET project in the field of innovative buildings, is that it adds value to the research of retrofiting

the existing buildings with innovative and collaborative solutions that can better assist in the quest for energy savings and emissions reductions. The demonstration of the KEToperation is made using an existing office building named Solar XXI, which was originally developed as a passive building with efficient solution sets and strategies [19]. Solar XXI building, which has a proven record of high performance with respect of zero energy concept [20], was “upgraded” in the context of this study with a set of connectivity technologies allowing for easy integration of multiple building systems and sharing of data and information, as shown later. This paper, therefore, hopes to provide insights on the energy needs and on thermal comfort benefits of adding smart building technologies into building operation, based on a case study in Portugal.

This paper is organised into four sections. The first section presents the framework and the goal of the research. The second section characterises the materials and methods, which include the case study, the control systems, the thermal comfort approach and the simulation and validation. The second section briefly discussed solar availability in the Portuguese context and compared it to other European contexts. The third section describes the findings in terms of thermal comfort and energy performance. Finally, the fourth section draws conclusions from the previous sections.

2. Materials and Methods

2.1. Case Study

The Solar XXI building, presented in Figure 1, was built in 2006 and belongs to the Portuguese National Laboratory of Energy and Geology’s (LNEG) energy laboratory headquarters and a real living laboratory demonstrator of a building nZEB performance [19]. The building is located in Lisbon and has an area of 1500 m², 1200 m² of which are heated, distributed by three floors containing offices, laboratories and test rooms. The Solar XXI building integrates several passive solutions that reduce energy needs, both for Winter and Summer, through window shading, natural lighting, the use of passive cooling from earth tubes and passive heating through BIPV [21].



Figure 1. Solar XXI building, LNEG—Lumiar campus, Lisbon (38°77' N–9°18'0'' W).

The constructive design of the building consists of the envelope solutions described in Table 1.

Table 1. Solar XXI thermal characteristics.

Building Component	Description (From Exterior Layer to Interior Layer)	U-Value [W/m ²]
Roof (gravel)	Gravel (5 cm), expanded polystyrene (5 cm), extruded polystyrene (5 cm), shaping layer (13 cm), reinforced concrete slab (20 cm), traditional plaster (2 cm)	0.342
Roof (slab)	Paving slabs (10 cm), expanded polystyrene (5 cm), extruded polystyrene (5 cm), shaping layer (18 cm), reinforced concrete slab (20 cm), traditional plaster (2 cm)	0.305
Exterior wall	Traditional plaster (3 cm), expanded polystyrene (6 cm), masonry (22 cm), traditional plaster (2 cm)	0.485
Interior wall	Traditional plaster (1 cm), masonry (11 cm), traditional plaster (1 cm)	3.525
Interior pavement	Concrete (30 cm), shaping layer (10 cm), linoleum (0.3 cm)	3.221
Ground pavement	Gravel (15 cm), extruded polystyrene (10 cm), concrete (15 cm), shaping layer (9 cm), linoleum (0.3 cm)	0.332
Windows	Double glazed aluminium window frames; SHGC = 0.63	2.943

Monitoring Laboratory

The monitored test room (Office104) was a 5.2 m × 3.4 m × 3.5 m test room purposed to be an office for one person. The test room had a window in the southern wall with an area of 2.5 m² shaded by an exterior Venetian blind to manage solar gains in the summer. The north wall connected the test room to the central corridor, and the remaining walls connected with other offices, illustrated by Figure 2. Above the door, there was an adjustable translucent vent that could be opened to control the office indoor air quality and allow heat exchange.



Figure 2. Solar XXI floor 1 blueprint: Test room location and building orientation.

The installed sensors allowed monitoring diverse aspects of the monitored room, such as temperature; relative humidity; carbon dioxide (CO₂) concentration, with a SED-CO₂-G-5045 [22]; and luminosity, with an ARGUS Presence Master with IR [23], which guided the implemented algorithms in the installed systems. An interface was located in the room where the user could assess the indoor air quality and alter the heating setpoint (SE8650U0B11 [24]). The SED-CO₂-G-5045 measured temperature with a ±0.3 °C accuracy, humidity with a ±3% accuracy, and CO₂ with a ±60 + 3% ppm accuracy, for a range of 0 to 5000 ppm [22]. The ARGUS Presence Master with IR detected illuminance within a range of 10 to 1000 lux [23]. Additionally, meteorological data were collected on-site through a weather station installed on the roof of Solar XXI [25].

The measured data were collected and stored through the EcoStruxure Power Monitoring Expert software platform by Schneider Electric [26], as shown in the example presented in Figure 3. This platform provides advanced energy visualisation and analysis

tools, enabling building audit, identify abnormal energy usage and patterns, and validate savings [26].

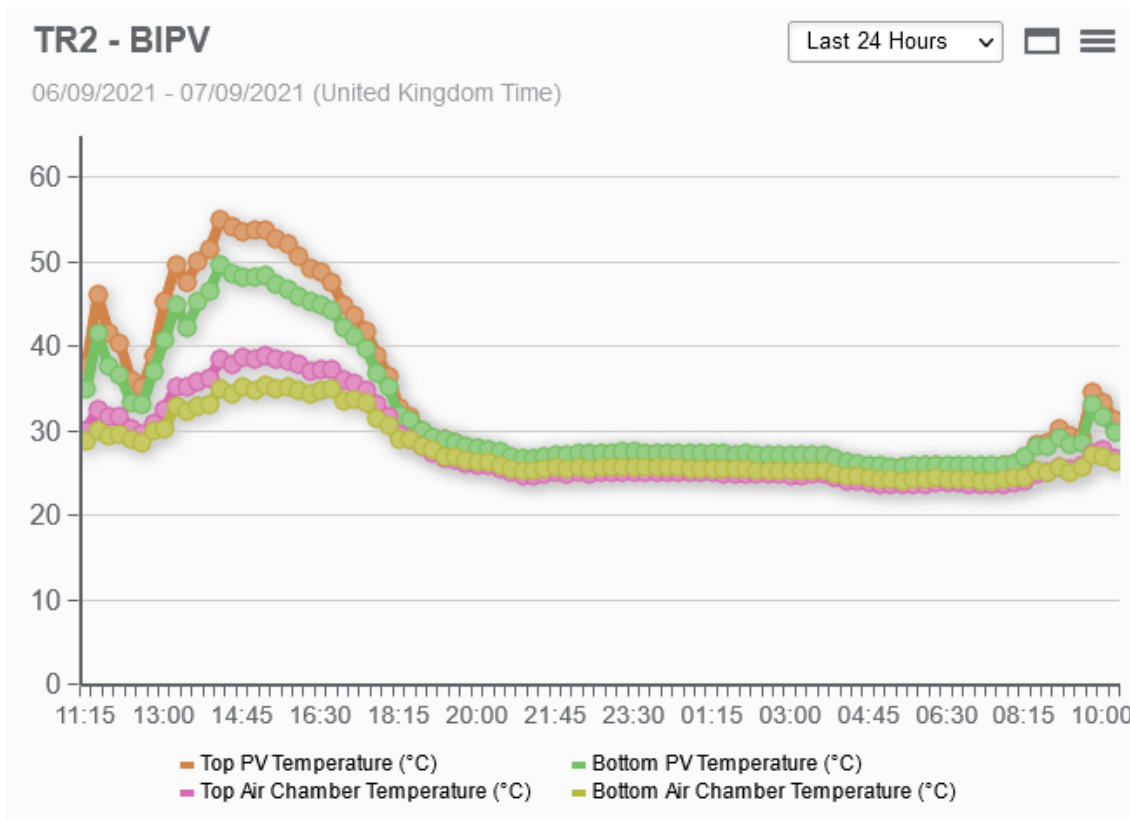


Figure 3. EcoStruxure Power Monitoring Expert interface.

2.2. Control Systems

For a building to attain nZEB status, it is required to have high energy performance by having low energy needs compensated heavily by local energy production from renewable sources. While the concept of SRI is being assessed by the European Commission [27,28], in this section, the integration of the control systems in the monitored test room is described, illustrated in Figure 4 and presented in Figure 5.

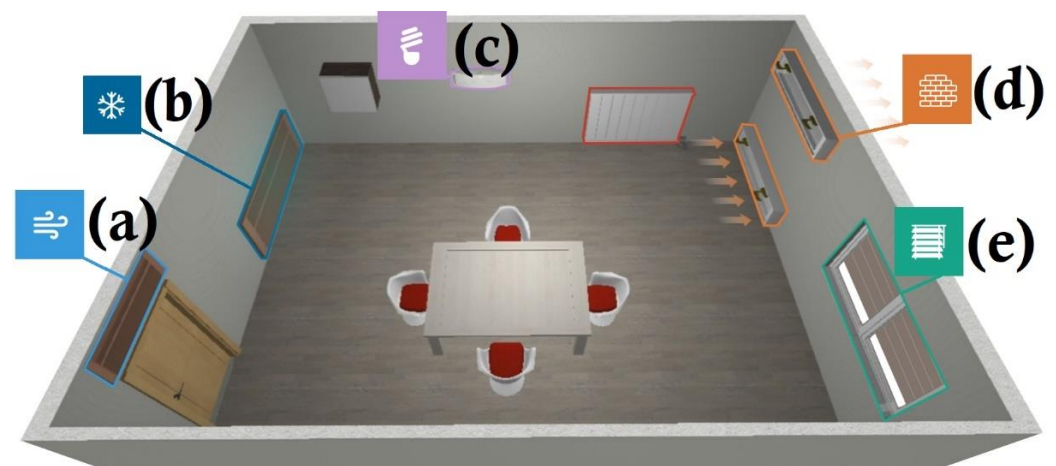


Figure 4. Schematic of the control systems in the test room: (a) Over-door air vent; (b) Earth tubes; (c) Light; (d) BIPV; (e) Blinds. HMI—EcoStruxure Building Operation interface [29].

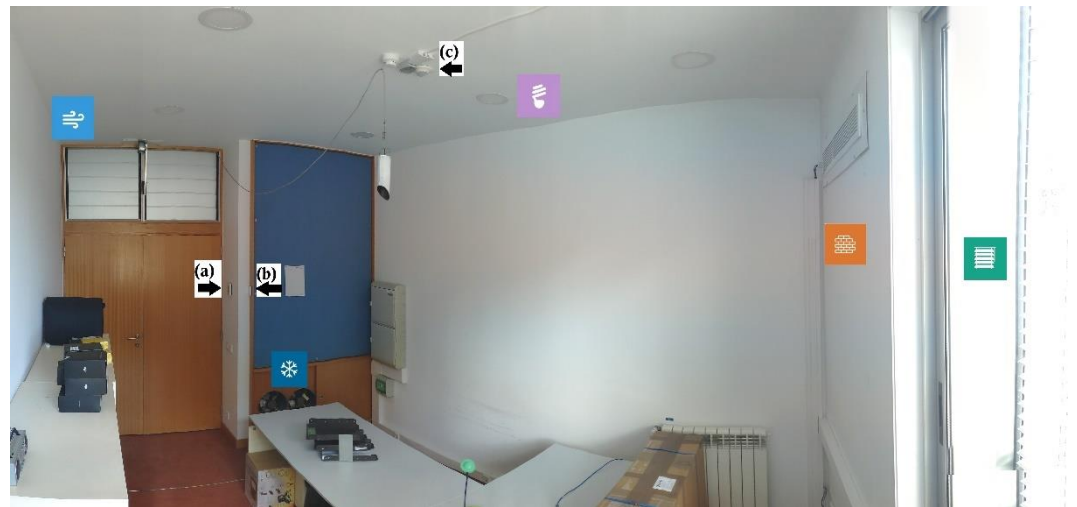


Figure 5. Test room: (a) SE8650U0B11 (Indoor air quality interface); (b) SED-CO2-G-5045 (Temperature, humidity, CO₂ sensor); (c) ARGUS Presence Master with IR (Light sensor).

2.2.1. BIPV

The Building-Integrated Photovoltaic (BIPV) systems were installed in the south façade of the Solar XXI building in 2006. These systems act as an outer shell to the current building envelope, which enables the reduction in thermal fluxes to the outdoors [30] and increase in thermal mass, which is characterised by having each an interior air cavity separating the building and the vertical PV cover (four BP3160 (160 W) [31] solar panels) and have four openings, two in the exterior (above and below the PV cover) and two in the interior (on the upper and lower section of the wall) which allow several airflow configurations. During PV operation, electric energy conversion generates heat, leading to high module temperatures [25,32,33]. The airflow configurations allow (natural or mechanical) ventilation to remove heat from the PV modules, leading to higher PV efficiencies [25,32,34–36] and reducing potential overheating while also potentially heating or removing heat from the indoor air space, as represented in Figure 6 [37].

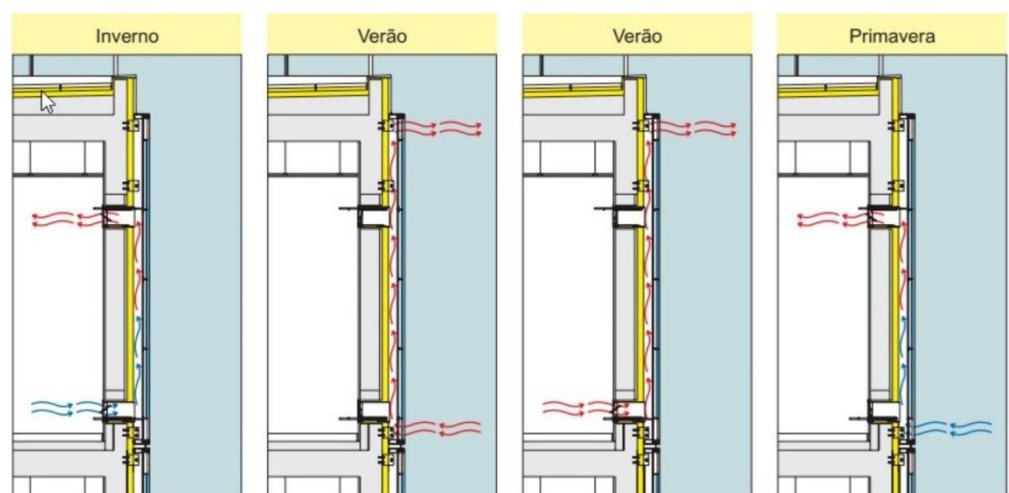


Figure 6. BIPV airflow configurations—from left to right, MOD1, MOD3, MOD4, MOD2.

In Figure 6, four configurations are described. The first configuration (MOD1), from left to right, uses the indoor air to cool the PV module and recovers the heated-up air to the indoor space, providing additional heating and is typically used to heat up the indoor space during occupation. The second configuration (MOD3) uses the outdoor air to cool

the PV modules. This configuration is used when the BIPV cannot be used to heat the indoor space nor aid in ejecting hot air from the indoor space. The third configuration (MOD4) allows heat to escape the building when cool air is being injected in the indoor space, through earth tubes or an over-door air vent. This configuration is used when the indoor air temperature is above comfortable levels. The last airflow configuration (MOD2) is an alternative to the first configuration, where outdoor air is used to cool the PV modules and is injected indoors. This configuration is used when the outdoor air temperature is higher than the indoor air temperature. For more details regarding the BIPV main features, please refer to [38].

The temperature within the BIPV air cavity is measured by two PT100 thermocouple probes, which operate for a range of -70 to 400 °C [39]. The detailed algorithm of the BIPV controlled operation is presented in Figure 7, and a fragment of the implemented algorithm in Figure 8, described in Tables 2 and 3, respectively.

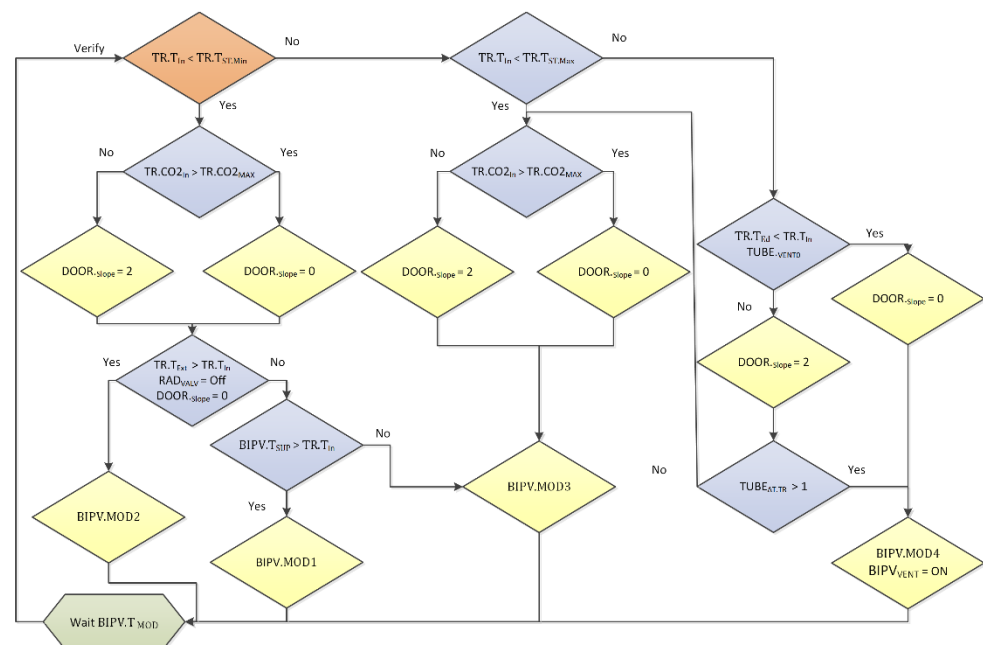


Figure 7. BIPV algorithm.

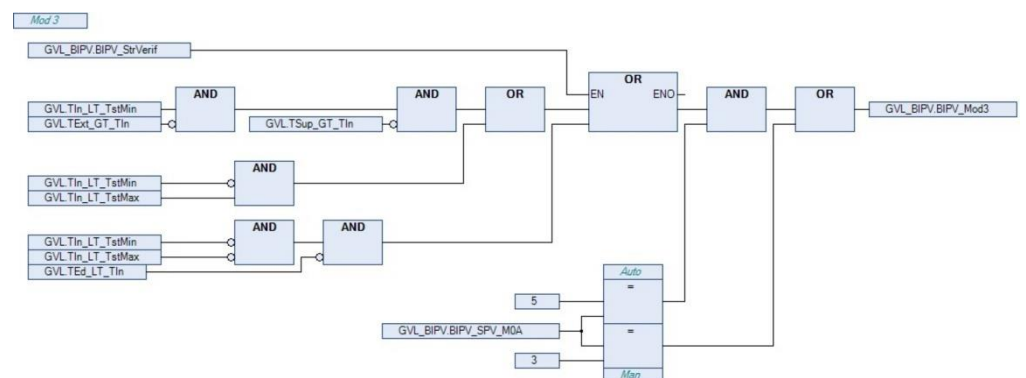


Figure 8. BIPV algorithm in EcoStruxure Machine Expert—MOD3.

Table 2. BIPV algorithm nomenclature.

Group	Parameter	Description
BIPV	MOD	Defines the BIPV operation mode as described in Figure 5
	T _{MOD}	User-defined minimum time interval of each operation mode
	T _{Sup}	Measured air cavity temperature at the top end of the BIPV
	Vent	Defines the operation of the fans in the BIPV air cavity
DOOR	Slope	Defines the slope of the over-door air vent; 2 = Vertical (Closed); 0 = Horizontal (Open)
RAD	VALV	Defines the operation of the radiator valve
TR	TCO ₂ In	Measured test room CO ₂
	TCO ₂ MAX	User-defined maximum CO ₂ setpoint
	T _{ed}	Measured corridor air temperature
	T _{ext}	Measured outdoor air temperature
	T _{in}	Measured test room air temperature
	T _{ST} ·Max	User-defined minimum test room air temperature setpoint
TUBE	T _{ST} ·Min	User-defined maximum test room air temperature setpoint
	Vent	Defines the velocity of the fans in the earth tubes; Vent0 = Off
	ΔT.TR	Evaluates the temperature differential between the test room air temperature and the earth tube air temperature

Table 3. BIPV algorithm nomenclature—EcoStruxure Machine Expert.

Parameter	Description
GVL	Global Variable List
GVL.BIPV	BIPV Global Variable List
BIPV_StrVerif	Verification start (Boolean)
BIPV_SPV_M0A	BIPV control mode; 5 = Automatic; 1,2,3,4 = Manual, corresponding to each BIPV operation mode defined in Figure 6 (Integer)
TEd_LT_TIn	Measured corridor air temperature lower than measured test room air temperature (Boolean)
TExt_GT_TIn	Measured outdoor air temperature greater than measured test room air temperature (Boolean)
TIn_LT_TstMax	Measured test room air temperature lower than user-defined maximum air temperature setpoint (Boolean)
TIn_LT_TstMin	Measured test room air temperature lower than user-defined minimum air temperature setpoint (Boolean)
TSup_GT_TIn	Measured air cavity temperature greater than measured test room air temperature (Boolean)

The algorithm is continuously assessing the system's thermal status (indoor air temperature, outdoor air temperature, earth tube temperature, air cavity temperature) to determine the ideal BIPV configuration.

2.2.2. Over-Door Air Vent

As described, above the office doors, there is an adjustable translucent vent of 1.15 m² which allows airflow between the office and the building through cross ventilation while also making use of the existing natural lighting strategies [21], presented in Figure 9. The vent operation is described in Figure 7, where it has a role of CO₂ management, opening the vent when the office CO₂ levels attain a defined maximum CO₂ concentration of 800 ppm, and also to guide airflow, whether to renew office air when hot air is being extracted, or to receive air from the office when it is being insufflated with outdoor air.



Figure 9. Over-door air vent.

2.2.3. Earth Tubes

Earth tubes use the ground to cool down outdoor air, allowing cool air to enter the offices when needed. The ground acts as a thermal sink, as Lisbon's outdoor air can reach 35 °C, while the ground floor temperature will be between 16 °C and 18 °C [37]. This system is more effective during the afternoon, as the outdoor air cools, but the indoor air remains high due to the building's thermal inertia. In the test room, there are two earth tube openings with a 0.15 m radius, which insufflates the office with captured outdoor air 15 m from the building, and redirects it through tubes that are buried 4.6 m underground, allowing heat exchange from the outdoor air with the soil through the tubes' cement walls [37]. For more details regarding the earth tubes, please refer to [38].

This system can prevent the passage of air, allow air to circulate naturally, or use fans to assist the office cooling. Each fan has a maximum airflow rate of 200 m³/h [40]. Each fan can operate for 5 different velocities, allowing 12 operational schemes: off, natural ventilation, and 10 mechanical ventilation schemes, allowing a maximum airflow rate of 400 m³/h.

The earth tubes entry in the office is presented in Figure 10.



Figure 10. Office earth tube opening.

The implemented earth tube algorithm evaluates the indoor air temperature and the possibility of the earth tube to aid heat/cool the office. If the office air temperature is

above the defined maximum temperature setpoint, the earth tubes will cool according to the difference between the current office air temperature and the maximum temperature setpoint, adjusting the fan speed to the office needs.

Earth tubes are also accounted for in the BIPV algorithm in Figure 7. As it provides cool air to the office, the BIPV configuration adapts to the configuration, which allows hot air to leave the office.

2.2.4. Lighting

Each office was equipped with an ARGUS Presence Master with IR [23], presented in Figure 5, mounted on the ceiling, which monitors the office illuminance, dimming the office lights in according to the office's luminous needs. The algorithm indicates the system to dim the lighting when the office luminosity is above a maximum setpoint of 500 lux and to increase the lighting when the office luminosity is below a minimum setpoint of 300 lux for each defined timestep while also verifying office occupancy.

2.2.5. Blinds

Solar XXI southern façade was equipped with Warema–Cruzfer Venetian blinds for each window, which can be adjusted vertically and whose blades' angle can be altered. The blades have 0.06 m width and are 0.055 m apart, distanced 0.33 m from the window. These blinds reduce the solar gains into the offices and prevent overheating during the summer, reflecting up to 80% of solar radiation [41]. The algorithm is designed, for temperatures below the minimum setpoint temperature, to raise the blinds to allow sunlight entry, in turn decreasing the artificial lighting needed. For temperatures between the minimum setpoint and the maximum setpoint temperature, the blinds control the office's illuminance to ensure sufficient illuminance and only act to reduce sunlight case the measured illuminance is too great. Lastly, for office air temperatures greater than the maximum temperature, the blinds act to block sunlight and minimise solar gains.

Furthermore, it is noteworthy to remark that the setpoints defined are not necessarily defined as comfort limits but can be adjusted to act before reaching comfort limits in order to prevent the comfort limit from being reached.

2.3. Thermal Comfort

Thermal comfort is defined as “the mental condition which expresses satisfaction with the thermal environment” [42]. According to Fanger [43], there are six main factors that influence occupant thermal comfort, four related to the thermal environment: air temperature, mean radiant temperature, relative air velocity, vapour pressure in the ambient air; and two related to the occupant: activity level and clothing thermal resistance. From these parameters, the Predicted Mean Vote (*PMV*) and Predicted Percentage Dissatisfied (*PPD*) are obtained. The *PMV* predicts the average response of a population according to the American Society of Heating, Refrigerating and A-C Engineers (ASHRAE) thermal sensation scale, where 0 is defined as “comfortable”, negative values as “cold” and positive values as “hot”, defined by Equation (1).

$$PMV = (0.303e^{-0.036M} + 0.028) \times L, \quad (1)$$

where *M* is the occupant metabolic heat generation (W/m^2) and *L* the occupant's thermal load (W/m^2), defined by Equation (2).

$$L = (M - W) - 3.96 \times 10^{-8} f_{cl} [(T_{cl} + 273)^4 - (\bar{T}_r + 273)^4] - f_{cl} h_c (T_{cl} - T_a) - 3.05 [5.73 - 0.007(M - W) - P_a] - 0.42 [(M - W) - 58.15] - 0.0173M(5.87 - P_a) - 0.0014M(34 - T_a), \quad (2)$$

where *W* is the effective mechanical power (W/m^2), often considered 0 for conservative results. f_{cl} represents the clothing area factor (dimensionless), T_{cl} is defined as the temperature of the outer surface of the occupant's clothes ($^{\circ}C$), \bar{T}_r is the mean radiant temperature ($^{\circ}C$) and T_a represents the ambient air temperature ($^{\circ}C$). The variable h_c de-

defines the convective heat transfer coefficient (W/m^2) and P_a defines the ambient air vapour pressure (kPa).

ASHRAE 55 [44] defines the occupant comfortable zone for PMV values between -0.5 and 0.5 . Similarly, PPD is a function of PMV , establishing the predicted percentage of the population unsatisfied with the thermal environment, defined in Equation (3).

$$PPD (\%) = 100 - 95e^{-(0.03353PMV^4 + 0.2179PMV^2)} \quad (3)$$

Converting the established comfortable zone defined between PMV values of -0.5 and 0.5 to PPD , the comfortable zone is defined for PPD values under 10%.

2.4. Simulation

The tools used in the building simulation were EnergyPlus Version 9.5 and SketchUp Make 2017. EnergyPlus is a building simulation tool used to model building energy consumption which allows an integrated evaluation of the building system [45]. EnergyPlus played an essential role in predicting the behaviour and impact of the implemented control systems, whose implementation was validated with on-site measured data. SketchUp is a 3D modelling program owned by Trimble Inc., which is used by architects, civil and mechanical engineers [46]. The SketchUp illustrated in Figure 11 represents the Solar XXI building.

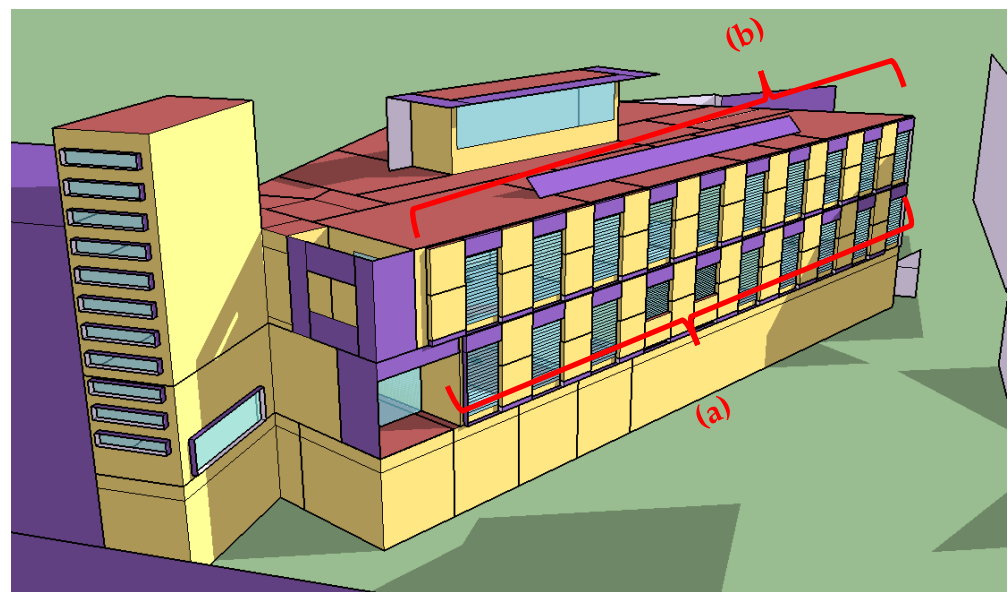


Figure 11. Solar XXI building (SketchUp model): (a) Floor 1: Corridor 0, test room and offices 101–108; (b) Floor 2: Corridor 1 and offices 201–208.

Input Data

Data and occupant behaviour observation were made in order to simulate the building operation. The studied office, despite unoccupied, was studied as occupied through simulation to assess the impact of the systems on occupant thermal comfort. The occupation schedule considered was similar to the occupancy schedule of the other occupants, Monday to Friday from 9:30 to 18:30, with a 2 h lunch break at 12:30. From ASHRAE [42], occupant metabolic heat generation was obtained ($65 W/m^2$, 120 W, office activity, typing) with summer clothing (0.5 clo) and winter clothing (1 clo) and a 24 h 20 W equipment with an additional 100 W resulting from occupant work activities and a lighting consumption of $8 W/m^2$ [47]. The Solar XXI building had no active cooling system, and the heating temperature was $20 ^\circ C$, provided by radiators. The air infiltration value used was 1.32 ACH (Air Changes per Hour) [48].

The control systems were implemented in EnergyPlus through the combination of individual schedules and the Energy Management System (EMS) tool, which allows adapting the schedules based on the result of the systems' algorithm. For example, the BIPV system was designed using the Zone Mixing tool in conjunction with EMS programs, permitting the design of multiple airflow configurations without overlap. The BIPV EMS programs, for each timestep, would set each BIPV Zone Mixing schedules to either 0 (Off) or 1 (On) based on the office indoor air temperature, the minimum and maximum setpoint temperatures, the outdoor air temperature, the building corridor air temperature and the office CO₂ concentration, as defined in Figure 7. For the earth tube system, the earth tube EMS program allowed to control the flow intensity for each timestep, multiplying the maximum airflow rate of 200 m³/h of each fan with the fraction obtained from the program, based on the temperature difference between the indoor air and the maximum setpoint temperature.

2.5. Validation

To validate the model, the measured temperature of each division of the building (corridors –1,0,1, offices 101–108, 201–208 and test room) was compared with the simulated temperature for homologous weather conditions. Furthermore, to evaluate the implemented BIPV algorithm in EnergyPlus, the temperature of the air cavity (TestroomBIPVInf and TestroomBIPVSup) was compared with the simulated results. To assess the building in similar weather conditions, the EnergyPlus weather file for Lisbon was altered with the atmospheric data measured on-site by the installed weather station on the roof of the Solar XXI building using the process described in [49]. Two statistical indexes were used to validate the model, the Mean Bias Error (*MBE*) and the Coefficient of the Variation of the Root Mean Square Error (*CvRMSE*), defined by Equations (4) and (5), adopted by ASHRAE and the Federal Energy Management Program (FEMP) [50,51], who suggest maximum values of 10% and 30%, respectively, for an hourly analysis.

$$MBE (\%) = \frac{\sum_i^n (S_i - M_i)}{\sum_i^n M_i} \times 100, \quad (4)$$

$$CvRMSE (\%) = \sqrt{\frac{\sum_i^n (S_i - M_i)^2}{\sum_i^n M_i}} \times 100, \quad (5)$$

where S_i and M_i represent the simulated and measured results for hour i , respectively, and n defines the period of analysis, in this case, 24 h.

In Figures 12 and 13, the obtained statistical indexes are presented, verifying the model's validity. As for the analysed period, all simulated thermal zones behave within the defined margin of error. Additionally, as the test room is the target of this study, Figure 14 presents the measured and simulated temperatures during the validation period.

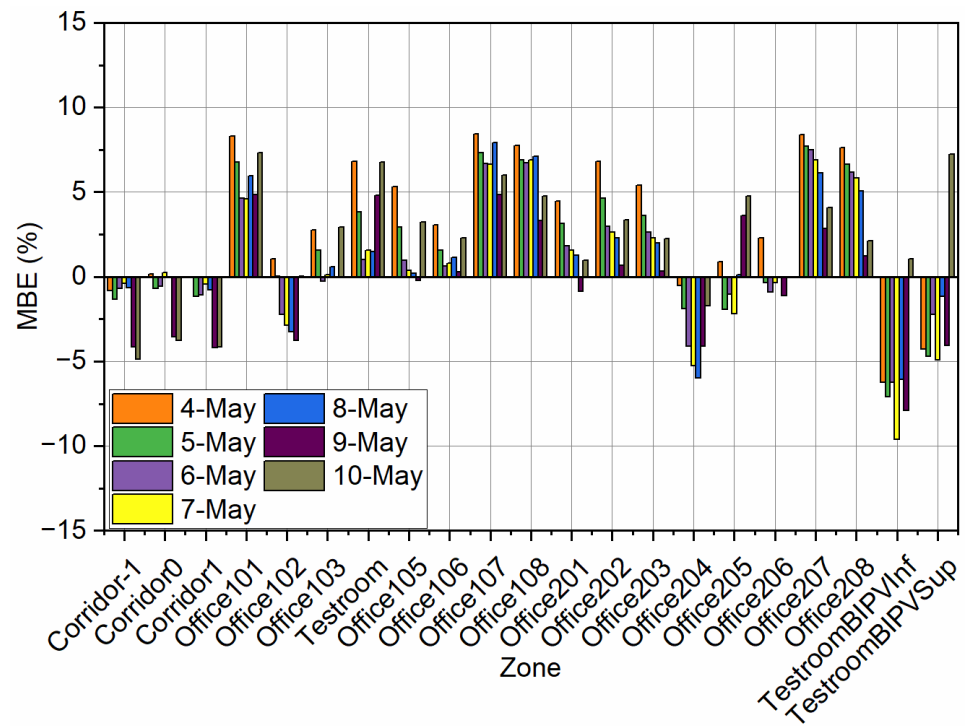


Figure 12. Building thermal zones MBE results.

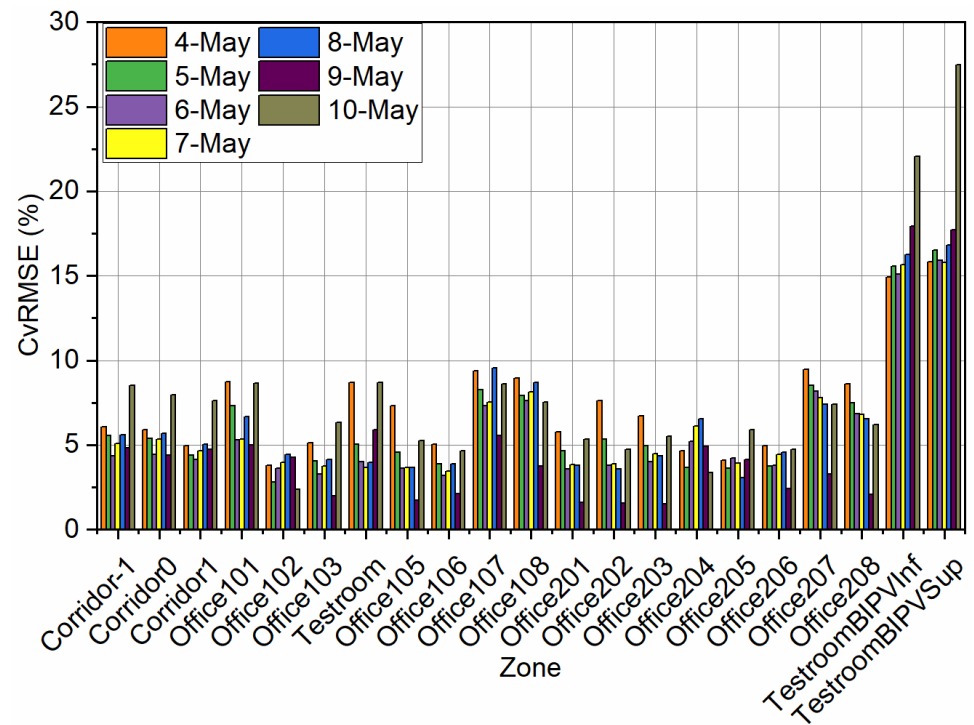


Figure 13. Building thermal zones CvRMSE results.

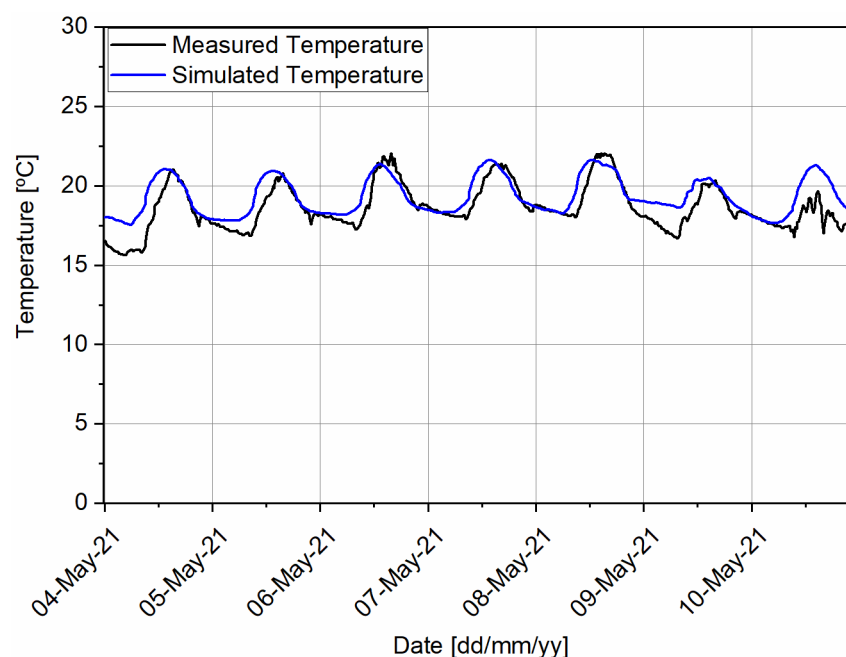


Figure 14. Test room thermal zone simulated temperature results.

3. Results and Discussion

In this section, the results of the simulated application of the control systems are presented. The building was evaluated through three models, which spawned from the validated model. The automatically controlled model applies the control systems to all applicable offices; the manually controlled model applies the control systems to all applicable offices, but with simulated human control; and the no KET model presents the building in a basic scenario with none of these systems. These models were evaluated, for winter and summer scenarios, on the test room thermal behaviour, on occupant thermal comfort, heating consumption and cooling needs.

For the automatic controlled system model, in order to reduce the building's dependency on active heating and cooling, the system setpoints were designed to prevent relying on active systems. As such, the minimum setpoint temperature was defined as 22 °C during the summer, as additional heating is undesired, and 23 °C otherwise, to maximise the usage of BIPV for indoor air heating. Conversely, the maximum setpoint temperature was defined as 25 °C during the summer to prevent overheating, and 24 °C otherwise.

For the manual controlled system, setpoints and system manual operation were designed under the assumption that occupants act when uncomfortable, in a corrective manner, and not a predictive manner. As such, the BIPV system operates under two regimes, MOD3 throughout summer and, for the non-summer months, MOD1 during the day and MOD3 during the night. The earth tubes were assumed to be manually actioned when the occupant felt hot (Temperature = 27 °C) and set to the maximum fan speed. The blinds were assumed to be fully open unless the maximum temperature is attained, where the occupant would close the blinds.

For the no KET model, the BIPV systems were removed, and the earth tubes turned off; however, the blinds remained under manual control.

For all models, the CO₂ algorithm and light algorithm functioned equally.

The detailed operation of each model is described in Table A1.

3.1. Thermal Comfort Performance

In a first analysis, the test room was evaluated with respect to its thermal performance. In this regard, two periods were analysed, January, representing winter conditions, and

August, representing summer conditions. The test room was assessed in terms of zone air temperature and occupant comfort.

3.1.1. Winter Scenario

To evaluate the performance of the implemented KETs in the winter scenario, the three models were compared for the month of January. In Figure 15, the zone air temperature for the three models is presented for weekdays (light orange shading) and weekends, where two tendencies can be observed: the test room with the KET systems had a lower temperature during nightfall; however, the KET systems provided with additional heating during occupation.

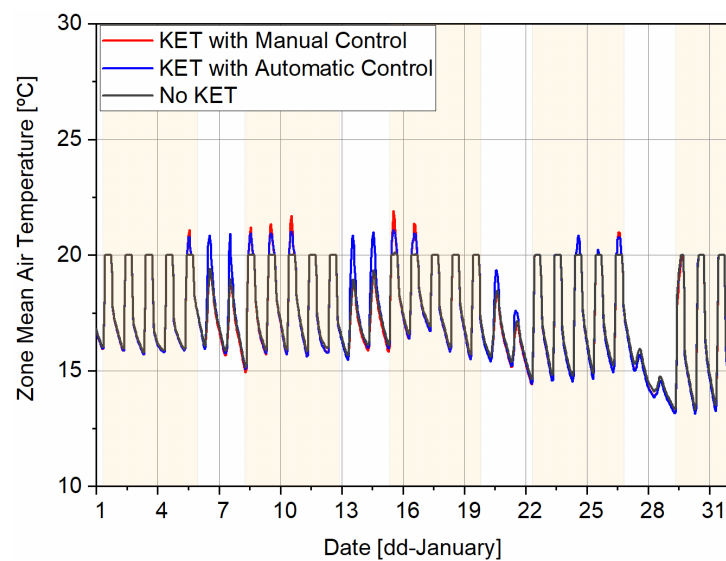


Figure 15. Test room winter thermal performance.

Figure 16 presents the simulated occupant comfort through *PMV* values during occupation (light orange shading), presenting results from 10:00 h to 18:00 h. The provided heating from the BIPV systems during occupation is reflected on the occupant thermal comfort, in Figure 16, where the models with the BIPV system and, consequently, the higher temperature during occupation led to improved occupant thermal comfort.

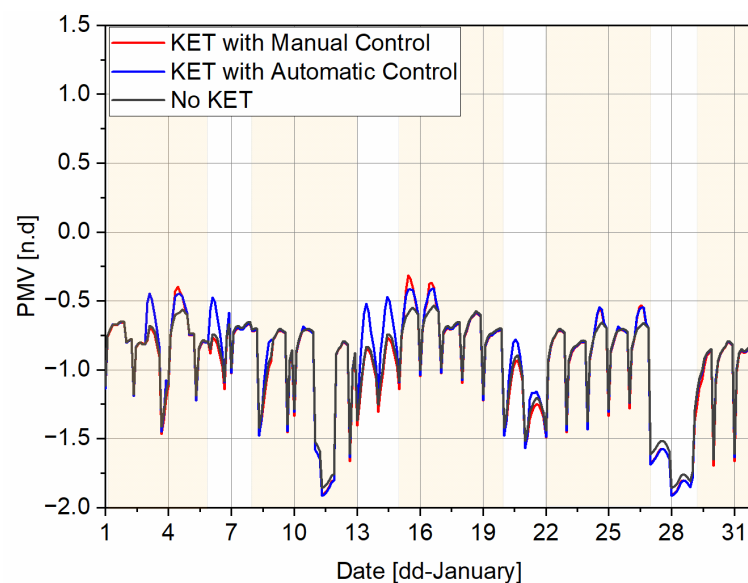


Figure 16. Test room winter occupant thermal comfort.

3.1.2. Summer Scenario

To evaluate the performance of the implemented KETs in the summer scenario, the three models were compared for the month of August. In Figure 17, the zone air temperature for the three models is presented for weekdays (light orange shading) and weekends, where two tendencies can be observed: The test room with the automatically controlled KET systems had a lower temperature throughout the month, registering 9 h over 27 °C, however, the manually controlled KET system led to poor results, due to the occupant's assumed corrective behaviour, attaining 153 h above 27 °C. Similarly, the test room without the KET systems attained high temperatures in the summer, with over 166 h above 27 °C.

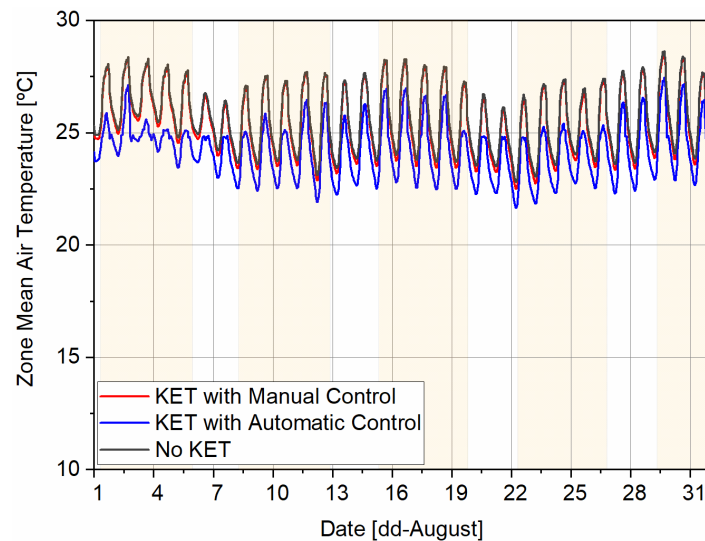


Figure 17. Test room summer thermal performance.

Figure 18 presents the simulated occupant comfort through *PMV* values during occupation (light orange shading). As mentioned for the analysed summer temperatures, the test room with the automatically controlled KET systems resulted in lower temperatures, reflected in the presented low *PMV* values, exceeding the $PMV = 0.5$ recommendation during 6 h of the analysed period, whereas the manually controlled model, which behaved poorly resulted in the higher *PMV* values, exceeding $PMV = 0.5$ for 97 h. The model without KET systems led to 108 h where the *PMV* is superior to 0.5.

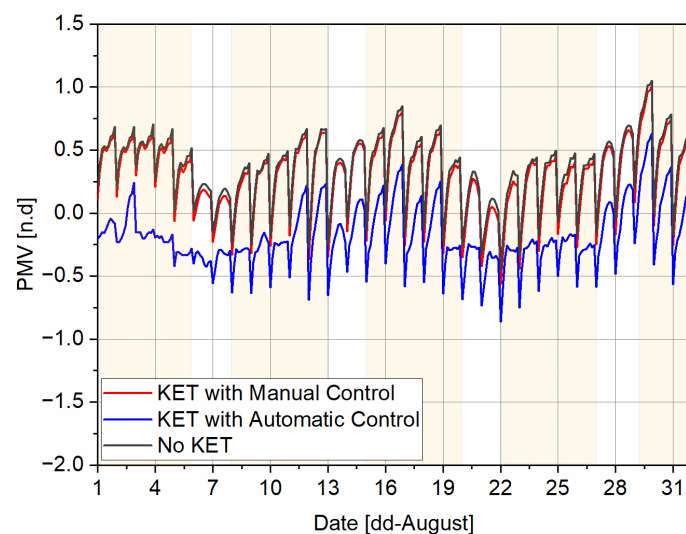


Figure 18. Test room summer occupant thermal comfort.

3.2. Energy Performance

As a consequence of the thermal behaviour of the test room, it is of interest to analyse the impact of the KET systems on the heating and cooling of the test room. An annual simulation of the three models and the heating consumption resulting from the radiator was created, and an ideal loads system to evaluate the cooling needs during the summer was implemented.

Figure 19 presents the test room's simulated heating consumption for the three models, where the impact of the KET systems on heating and the impact of automatic control over a manual control can be observed. The yearly estimated heating consumption for the automatically controlled system is of 179 kWh/year, or 10.2 kWh/m²/year, registering a reduction of 8.4% when compared to the manually controlled system and a reduction of 22.3% when compared to the model without the KET systems.

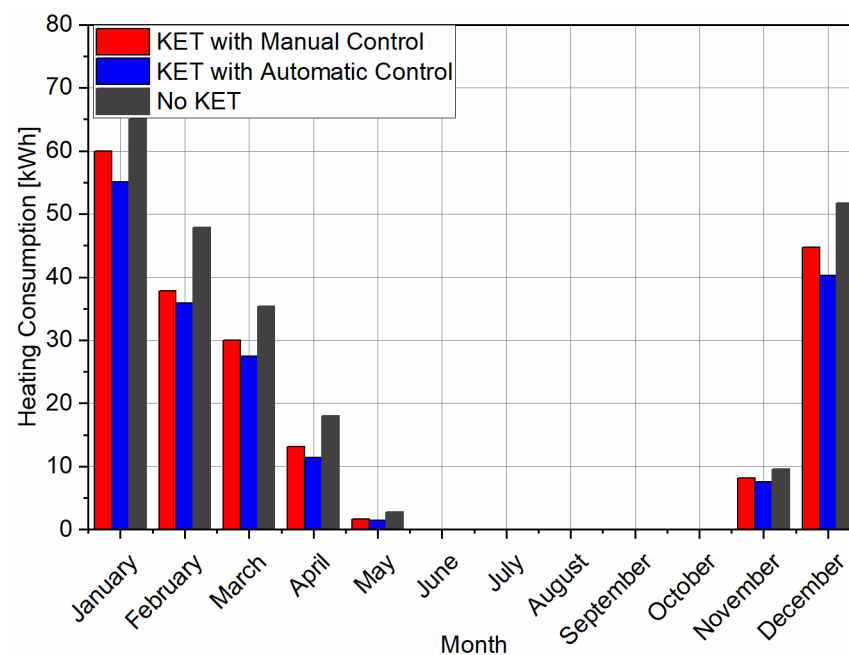


Figure 19. Test room annual heating consumption.

Figure 20 presents the test room's performance during the cooling period for the three models, where the impact of the KET systems on cooling prevention (in red and blue lines) and cooling needs (in columns) can be observed. The manually controlled system, due to its higher temperatures and assumed occupant corrective behaviour, led to increased cooling needs, as the earth tubes would only act to aid the cooling and not to prevent cooling, presenting simulated cooling needs of 19.46 kWh/year. Likewise, the model without the KET systems registers increased cooling needs, as it does not have the contribution of the earth tube, registering simulated cooling needs of 23.99 kWh/year. The test room's cooling needs for the automatically controlled KET model is estimated to be 0.75 kWh/year, as the room hardly surpassed the maximum temperature of 27 °C, due to the cooling provided by the earth tubes in advance, showcased by the blue line. In this scenario, the earth tubes provided 71 kWh cooling throughout the year. The contribution of the earth tubes allowed the automatically controlled model to attain cooling needs 97% lower than the other models, presenting a reduction of 1.33 kWh/m²/year when compared to the no KET model, highlighting their effectiveness in cooling prevention.

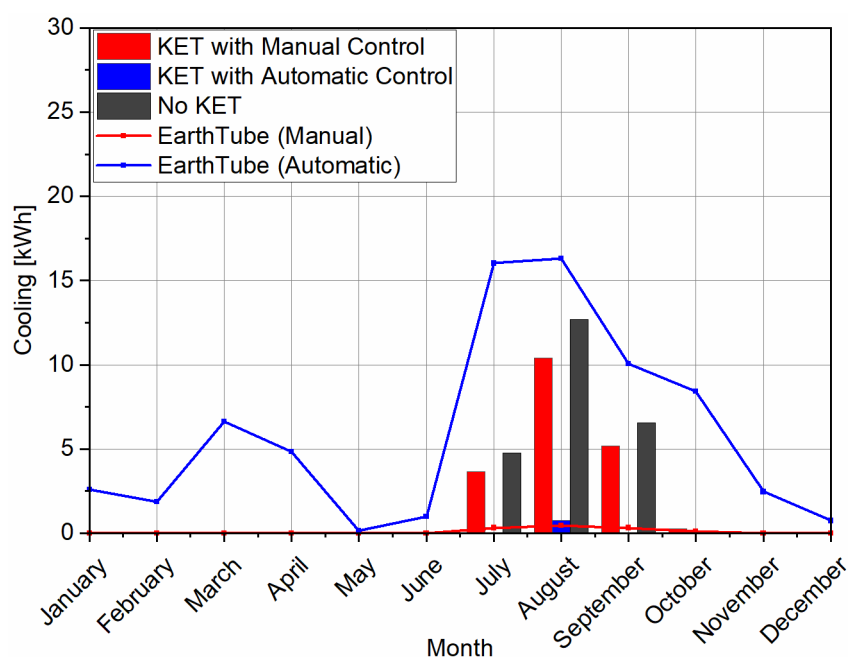


Figure 20. Test room annual cooling needs.

4. Conclusions

In this research, the application of Key Enabling Technologies in a monitored test room was evaluated through simulation regarding the improvement of control systems on the test room's thermal and energetic performance. This investigation is part of the SUDOKET project, which is committed to the application of KETs in the design and construction of innovative buildings, increasing efficiency and competitiveness of the building sector while reducing environmental impact.

A model of the Solar XXI building was created and validated through temperature comparison with the sensors placed in each thermal zone. From the validated model, three new models were created. A first model would simulate the building under normal operating conditions with all control systems installed where applicable, a second model, similar to the first, would represent the operation of the same systems, albeit with simulated manual control, and lastly, a third model which would remove the BIPV and the earth tubes systems, and manual blinds control. The comparison of these three models would allow retrieving insights into the impact of the systems and their control on the thermal and energetic performance of the test room.

For winter conditions, it was observed that the manually controlled system would behave similarly to the automatically controlled system and both systems would lead to an increase in temperature of the test room during occupation, reducing discomfort. Through a yearly analysis, the automatically controlled system model would require 22% less heating than the no KET model and 8% less heating than the manually controlled system model.

For summer conditions, as Solar XXI is a building with advanced building envelope solutions and high thermal inertia, it was seen that, for a cooling setpoint of 27 °C, the test room would require low cooling. However, due to the implementation of an earth tube algorithm that would prevent the test room from reaching 27 °C, the automatically controlled system would reduce cooling needs and improve occupant thermal comfort. By analysing the cooling needs throughout the year, it was observed that the automatically controlled systems would lead to a 97% cooling needs reduction when compared to the no KET model. In this analysis, the manually controlled system performed poorly due to the corrective nature of the manual algorithms when compared to the preventive nature of the automatic algorithms.

This work provides additional insights into the benefits of the indicated systems and the benefits of a designed automatically controlled system on occupant thermal comfort and test room acclimatisation needs. While this work focused on thermal comfort and energy performance benefits, the indicated systems also control indoor air quality through CO₂ and illuminance monitoring, having a more expansive role and contribution to smart buildings.

Author Contributions: Conceptualisation, L.A., J.F. and H.G.; methodology, L.A. and J.M.L.; validation, J.M.L.; formal analysis, J.M.L. and L.A.; investigation, L.A. and J.F.; resources, J.F. and H.G.; data curation, J.M.L.; writing—original draft preparation, J.M.L.; writing—review and editing, J.M.L., L.A., J.F., J.M.P. and D.A.; supervision, L.A. and J.F.; project administration, L.A., J.F., H.G., J.M.P. and D.A.; funding acquisition, J.F. and H.G. All authors have read and agreed to the published version of the manuscript.

Funding: This research was funded by SUDOKET—SOE2/P1/E0677—mapping, consolidation and dissemination of the Key Enabling Technologies (KETs) for the construction sector in the SUDOE space, funded by the INTERREG SUDOE cooperation program and co-financed by European Regional Development Funds (ERDF).

Institutional Review Board Statement: Not applicable.

Informed Consent Statement: Not applicable.

Data Availability Statement: The data presented in this study are available on request from the corresponding author.

Acknowledgments: This research was funded by SUDOKET—mapping, consolidation and dissemination of the Key Enabling Technologies (KETs) for the construction sector in the SUDOE space, funded by the INTERREG SUDOE cooperation program and co-financed by European Regional Development Funds (ERDF).

Conflicts of Interest: The authors declare no conflict of interest.

Appendix A

Table A1. Simulation model description.

System	No KET	KET-Manual Control	KET-Automatic Control
BIPV	[Non-existent]	Based on the time of the year. Summer: MOD3 Winter: Day: MOD1; Night: MOD3	Based on algorithm presented in Figure 7. Temperature setpoints Summer: 22–25 °C Winter: 23–24 °C CO ₂ setpoint: 800 ppm
Blinds	Based on indoor air temperature. Temperature < maximum temperature, Blinds fully open Temperature > maximum temperature, Blinds fully closed. Maximum temperature. Summer: 27 °C Winter: 24 °C	Based on indoor air temperature. Temperature < maximum temperature, Blinds fully open Temperature > maximum temperature, Blinds fully closed. Maximum temperature. Summer: 27 °C Winter: 24 °C	Algorithm based on indoor air temperature, illuminance and radiation setpoints. Maximum temperature. Summer: 25 °C Winter: 24 °C Illuminance setpoint. Maximum: 1000 lux Radiation setpoints. Vertical slats: 1000 W/m ² Oblique slats: 800 W/m ²
Over-Door air vent	Open for indoor CO ₂ level greater than 800 ppm		
Earth Tube	[Non-existent]	Based on indoor air temperature. Flow rate = 400 m ³ /h for indoor air temperature > 27 °C	Algorithm: Fan rotation velocity in function of the difference between the maximum indoor air temperature setpoint and the indoor air temperature. Flow rate = [0,400] m ³ /h Maximum temperature. Summer: 25 °C Winter: 24 °C
Lighting	8 Watts/m ² with stepped daylighting. Illuminance setpoint of 500 lux		

References

1. European Commission. New Rules for Greener and Smarter Buildings Will Increase Quality of Life for All Europeans. 2019. Available online: https://ec.europa.eu/info/news/new-rules-greener-and-smarter-buildings-will-increase-quality-life-all-europeans-2019-apr-15_en (accessed on 23 July 2021).
2. European Parliament. Directive 2010/31/EU of the European Parliament and of the Council of 19 May 2010 on the Energy Performance of Buildings. 2010. Available online: <https://eur-lex.europa.eu/eli/dir/2010/31/oj> (accessed on 26 February 2021).
3. Aelenei, L.; Petran, H.; Tarrés, J.; Riva, G.; Ferreira, A.; Camelo, S.; Corrado, V.; Šijanec-Zavrl, M.; Stegnar, G.; Gonçalves, H.; et al. New Challenge of the Public Buildings: nZEB Findings from IEE RePublic_ZEB Project. *Energy Procedia* **2015**, *78*, 2016–2021. [CrossRef]
4. Aelenei, L.; Paduos, S.; Petran, H.; Tarrés, J.; Ferreira, A.; Corrado, V.; Camelo, S.; Polychroni, E.; Sfakianaki, K.; Gonçalves, H.; et al. Implementing Cost-optimal Methodology in Existing Public Buildings. *Energy Procedia* **2015**, *78*, 2022–2027. [CrossRef]
5. Smart Readiness Indicator for Buildings. Available online: <https://smartreadinessindicator.eu/> (accessed on 23 July 2021).
6. European Commission. Commission Recommendation (EU) 2016/1318. 2016. Available online: <https://eur-lex.europa.eu/legal-content/EN/TXT/?uri=CELEX%3A32016H1318> (accessed on 26 February 2021).
7. European Commission. Horizon 2020 in Brief. The EU Framework Programme for Research & Innovation. 2014. Available online: https://ec.europa.eu/programmes/horizon2020/sites/default/files/H2020_inBrief_EN_FinalBAT.pdf (accessed on 23 July 2021).
8. SudoKET. What Are KETs? 2018. Available online: <http://ketpedia.com/what-are-kets> (accessed on 23 July 2021).
9. Ma, Z.; Paul, C.; Daly, D.; Ledo, L. Existing building retrofits: Methodology and state-of-the-art. *Energy Build.* **2012**, *55*, 889–902. [CrossRef]
10. Ascione, F.; Bianco, N.; Iovane, T.; Mastellone, M.; Mauro, G.M. Conceptualization, development and validation of EMAR: A user-friendly tool for accurate energy simulations of residential buildings via few numerical inputs. *J. Build. Eng.* **2021**, *44*, 102647. [CrossRef]
11. Santamouris, M.; Pavlou, C.; Doukas, P.; Mihalakakou, G.; Synnefa, A.; Hatzibiros, A.; Patargias, P. Investigating and analysing the energy and environmental performance of an experimental green roof system installed in a nursery school building in Athens, Greece. *Energy* **2007**, *32*, 1781–1788. [CrossRef]
12. Chidiac, S.; Catania, E.; Morofsky, E.; Foo, S. Effectiveness of single and multiple energy retrofit measures on the energy consumption of office buildings. *Energy* **2011**, *36*, 5037–5052. [CrossRef]
13. Menezes, A.C.; Cripps, A.; Bouchlaghem, D.; Buswell, R. Predicted vs. actual energy performance of non-domestic buildings: Using post-occupancy evaluation data to reduce the performance gap. *Appl. Energy* **2012**, *97*, 355–364. [CrossRef]
14. Turner, C.; Frankel, M. *Energy Performance of LEED® for New Construction Buildings*; U.S. Green Building Council; New Buildings Institute: White Salmon, WA, USA, 2008.
15. Owens, J.; Wilhite, H. Household energy behavior in Nordic countries—An unrealized energy saving potential. *Energy* **1988**, *13*, 853–859. [CrossRef]
16. Dong, B.; Prakash, V.; Feng, F.; O’Neill, Z. A review of smart building sensing system for better indoor environment control. *Energy Build.* **2019**, *199*, 29–46. [CrossRef]
17. Reinhart, C.F.; Voss, K. Monitoring manual control of electric lighting and blinds. *Light. Res. Technol.* **2003**, *35*, 243–258. [CrossRef]
18. SudoKET. SUDOKET Project. 2018. Available online: <http://en.sudoket.com/project> (accessed on 23 July 2021).
19. Aelenei, L.; Gonçalves, H. From Solar Building Design to Net Zero Energy Buildings: Performance Insights of an Office Building. *Energy Procedia* **2014**, *48*, 1236–1243. [CrossRef]
20. Aelenei, D.; Lopes, R.A.; Aelenei, L.; Gonçalves, H. Investigating the potential for energy flexibility in an office building with a vertical BIPV and a PV roof system. *Renew. Energy* **2019**, *137*, 189–197. [CrossRef]
21. Gonçalves, H.; Aelenei, L.; Rodrigues, C. Solar XXI: A Portuguese office building towards net zero-energy building. *REHVA Eur. HVAC J.* **2012**, *49*, 34–40.
22. Schneider Electric. Wireless CO₂ Sensor with Room Temperature and Humidity for SE8000 Series, Zigbee Communication Protocol. Available online: <https://www.se.com/ww/en/product/SED-CO2-G-5045/wireless-co2-sensor-with-room-temperature-and-humidity-for-se8000-series%2C-zigbee-communication-protocol/> (accessed on 27 August 2021).
23. Schneider Electric. Argus Presence Master with IR, Relay 2-Gang, Polar White. 2021. Available online: <https://www.se.com/ww/en/product/MTN5510-1219/argus-presence-master-with-ir%2C-relay-2-gang%2C-polar-white/> (accessed on 23 July 2021).
24. Schneider Electric. Roof Top Unit, Heat Pump & Indoor Air Quality Ctrl: BACnet MS/TP, RH Sensor & Control, White Case/Fascia. Available online: <https://www.se.com/ww/en/product/SE8650U0B11/roof-top-unit%2C-heat-pump-%26-indoor-air-quality-ctrl%3A-bacnet-ms-tp%2C-rh-sensor-%26-control%2C-white-case-fascia/> (accessed on 27 August 2021).
25. Lourenço, J.M.; Aelenei, L.; Sousa, M.; Facão, J.; Gonçalves, H. Thermal Behavior of a BIPV Combined with Water Storage: An Experimental Analysis. *Energies* **2021**, *14*, 2545. [CrossRef]
26. Schneider Electric. ExoStruxure Power Monitoring Expert. Available online: <https://www.se.com/ww/en/product-range/6540-4-ecostruxure-power-monitoring-expert/#overview> (accessed on 2 August 2021).
27. Energy Performance of Buildings Concerted Action. CT6 Smart Buildings. 2021. Available online: <https://epbd-ca.eu/topics-teams/topics/ct-6-smart-buildings> (accessed on 23 July 2021).

28. Publications Office of the EU. Final Report on the Technical Support to the Development of a Smart Readiness Indicator for Buildings. Available online: <https://op.europa.eu/en/publication-detail/-/publication/bed75757-fbb4-11ea-b44f-01aa75ed71a1/language-en> (accessed on 23 July 2021).
29. Schneider Electric. EcoStruxure Building Operation. Available online: <https://www.se.com/ww/en/product-range/62111-ecostruxure%E2%84%A2-building-operation/> (accessed on 25 August 2021).
30. Gagliano, A.; Aneli, S. Analysis of the energy performance of an Opaque Ventilated Façade under winter and summer weather conditions. *Sol. Energy* **2020**, *205*, 531–544. [CrossRef]
31. Solar Design Tool. BP BP3160 (160W) Solar Panel. Available online: <http://www.solardesigntool.com/components/module-panel-solar/BP/3268/BP3160/specification-data-sheet.html> (accessed on 23 July 2021).
32. Aelenei, L.; Pereira, R.; Gonçalves, H. BIPV/T versus BIPV/T-PCM: A numerical investigation of advanced system integrated into Solar XXI building façade. In Proceedings of the 2nd International Conference on Sustainable Energy Storage, Dublin, Ireland, 19–21 June 2013.
33. Agrawal, B.; Tiwari, G.N. Optimizing the energy and exergy of building integrated photovoltaic thermal (BIPVT) systems under cold climatic conditions. *Appl. Energy* **2010**, *87*, 417–426. [CrossRef]
34. Tina, G.M.; Scavo, F.B.; Aneli, S.; Gagliano, A. Assessment of the electrical and thermal performances of building integrated bifacial photovoltaic modules. *J. Clean. Prod.* **2021**, *313*, 34–40. [CrossRef]
35. Sousa, M.A.C.; Aelenei, L.; Gonçalves, H. Comportamento térmico de um protótipo BIPV combinado com armazenamento de água: Análise experimental. In *CIES2020: As Energias Renováveis na Transição Energética: Livro de Comunicações do XVII Congresso Ibérico e XIII Congresso Ibero-Americano de Energia Solar*; Gonçalves, H., Romero, M., Eds.; LNEG: Lisboa, Portugal, 2020; pp. 1167–1174.
36. Tina, G.M.; Scavo, F.B.; Gagliano, A. Multilayer Thermal Model for Evaluating the Performances of Monofacial and Bifacial Photovoltaic Modules. *IEEE J. Photovolt.* **2020**, *10*, 1035–1043. [CrossRef]
37. Edifício Solar XXI. 2005. Available online: https://repositorio.lneg.pt/bitstream/10400.9/1321/1/BrochuraSolarXXI_Dezembro2005.pdf (accessed on 29 July 2021).
38. Solar XXI towards Zero Energy. 2010. Available online: https://repositorio.lneg.pt/bitstream/10400.9/1322/1/BrochuraSolarXXI_Maio2010.pdf (accessed on 27 August 2021).
39. Amazon. Generic Rtd Pt100 Temperature Sensor 2M Cable Probe 50 Mm 3 Wires –50–400 Degree. Available online: <https://www.amazon.in/Generic-Pt100-Temperature-Sensor-50-400Degree/dp/B07KV34WZK> (accessed on 27 August 2021).
40. Pano, M.; Gonçalves, H. Solar XXI building: Proof of concept or a concept to be proved? *Renew. Energy* **2011**, *36*, 2703–2710. [CrossRef]
41. Catálogo Proteção Solar. Available online: <https://www.cruzfer.pt/pdf/Cat.%20P.%20Solar%202016.pdf> (accessed on 26 August 2021).
42. ASHRAE. Chapter 9—Thermal Comfort. In *2017 ASHRAE Handbook: Fundamentals*; ASHRAE, Ed.; ASHRAE: Atlanta, GA, USA, 2017; pp. 180–212.
43. Fanger, P.O. Assessment of man’s thermal comfort in practice. *Occup. Environ. Med.* **1973**, *30*, 313–324. [CrossRef]
44. Wikipedia. ASHRAE 55. 2021. Available online: https://en.wikipedia.org/wiki/ASHRAE_55 (accessed on 23 July 2021).
45. EnergyPlus. 2021. Available online: <https://www.energyplus.net> (accessed on 23 July 2021).
46. Wikipedia. SketchUp. 2021. Available online: <https://en.wikipedia.org/wiki/SketchUp> (accessed on 23 July 2021).
47. BuildUp. Edifício Solar XXI. Lisbon, Portugal, 2009. Available online: <https://www.buildup.eu/en/practices/cases/edificio-solar-xxi-lisbon-portugal> (accessed on 23 July 2021).
48. Bot, K.; Aelenei, L.; Gomes, M.d.G.; Santos Silva, C. Performance Assessment of a Building Integrated Photovoltaic Thermal System in Mediterranean Climate—A Numerical Simulation Approach. *Energies* **2020**, *13*, 2887. [CrossRef]
49. Pereira, J.O. Simulação Energética de Películas em Envidraçados. Master’s Thesis, University of Lisbon, Lisbon, Portugal, November 2015.
50. ASHRAE. *ASHRAE Guideline 14-2014: Measurement of Energy Demand and Water Savings*; American Society of Heating, Refrigerating and Air-Conditioning Engineers: Atlanta, GA, USA, 2014.
51. FEMP. Federal Energy Management Program. In *M&V Guidelines: Measurement and Verification for Performance-Based Contracts*; Version 4.0; U.S. Department of Energy Federal Energy Management Program: Washington, DC, USA, 2015.